SAE International™

Coordinated Electric Supercharging and Turbo-Generation for a Diesel Engine

2010-01-1228
Published
04/12/2010

Prasad Sajjan Divekar, Beshah Ayalew and Robert Prucka
Clemson Univ.

ABSTRACT

Exhaust gas turbo-charging helps exploit the improved fuel efficiency of downsized engines by increasing the possible power density from these engines. However, turbo-charged engines exhibit poor transient performance, especially when accelerating from low speeds. In addition, during low-load operating regimes, when the exhaust gas is diverted past the turbine with a waste-gate or pushed through restricted vanes in a variable geometry turbine, there are lost opportunities for recovering energy from the enthalpy of the exhaust gas. Similar limitations can also be identified with mechanical supercharging systems.

This paper proposes an electrical supercharging and turbo-generation system that overcomes some of these limitations. The system decouples the activation of the air compression and exhaust-energy recovery functions using a dedicated electrical energy storage buffer. Its main attributes fast speed of response to load changes and flexibility of control. A causal simulation model of the proposed system, including that of the Diesel engine, electrically driven compressor, energy buffer battery and power electronics, and the turbo-generation system are developed and analyzed. A coordinated control scheme is then implemented for the electric compressor and turbo-generator considering load demand fluctuations on the engine and enforcing battery state of charge constraints. The proposed system is evaluated on standard test cycles and compared with conventional turbo-chargers. The results show the potential of the system in improving transient performance, in general, and the cycle equivalent fuel efficiency over a standard city driving cycle.

1. INTRODUCTION

Strict government regulations and increasing energy costs continue to push manufacturers towards the development of more efficient automotive engines with reduced emissions. Furthermore, increasing efficiency by reducing fuel consumption remains the main, if not the only, way to meaningfully reduce CO_2 emissions and global warming. One of the established means to reduce fuel consumption without compromising steady-state torque capability is to downsize engines and fit them with superchargers or turbo-chargers to recover power density [1]. Most passenger cars with naturally aspirated engines utilize less than 10% of their rated engine power in most driving conditions [2]. Smaller/ downsized engines allow a larger area of their operating range to be more efficiently utilized for most of the time since the average engine operating points become closer to the minimum brake specific fuel consumption (bsfc) point of the engine. However, some type of supercharging or exhaust gas turbo-charging system should be available when high torque is demanded from the engine, e.g. for accelerating in a passing maneuver.

The major disadvantage with exhaust gas turbo-charging is the so-called the “turbo-lag” phenomena. Turbo-lag is caused by the fact that changes in driver demanded torque do not immediately reflect in the mass flow rate across the compressor (or the engine boost pressure and thereby, the output torque). Rather, the turbo-charger inertia must first be accelerated via the turbine whose torque output, in turn, depends on the mass flow rate and the thermodynamic state of the exhaust gases. This sequence leads to the identified turbo-lag effect on the transient response of the engine to demanded torque. Often, to accelerate the turbine faster, the upstream pressure is varied using variable geometry turbines (VGT); but these have the drawback of increasing exhaust back pressure and therefore the pumping losses of the engine. Furthermore, in operating regimes where the waste-gate diverts flow past the turbine or the control vanes in a VGT are manipulated to control turbine/compressor over-speed, most of the energy in the exhaust gases is not recovered. With

mechanical superchargers, similar transient response limitations arise since the compressor is mechanically coupled to the engine crankshaft whose speed is a response to in-cylinder combustion processes and affected by all connected inertia (including the step-up gearing for the compressor). There is also an added fuel penalty from the fact that the supercharging compressor is driven from the output of the engine itself.

The transient performance limitations and the lost opportunities to optimize energy use with either of these systems can be overcome by running the intake-boost system independent of the exhaust-recovery system. This requires drive systems coupled with an energy buffer (e.g. electric batteries or pneumatic accumulators) that supplies power for the compressor drive and absorbs power re-generated from the exhaust, thereby effectively decoupling the intake and exhaust sides. In this regard, some work has been done in incorporating electric motors and generators in the air flow path of IC Engines. In [3,4,5,6] air compressors driven by electric machines (electric superchargers) have been proposed to provide boost on the air intake side. Exhaust mounted electric turbines (Turbo-generators) discussed in [7, 8] can help recover a certain amount of the exhaust energy which otherwise gets wasted to the ambient as heat. The recovered energy can be used to re-charge the buffer battery.

This paper outlines a scheme to decouple the intake-boost system from the exhaust recovery system using electric supercharging and turbo-generation with two separate electric machines and a dedicated energy storage buffer/battery. The two electric machines are selected to satisfy their respective dynamic response and operating requirements. The schematic of the proposed system is shown in Figure 1 below. The electric supercharger provides boost level that can be independently and rapidly varied in response to the demand on the engine. When the electric supercharger is turned off, the engine runs naturally aspirated via a wide-open bypass valve. The turbo-generator recharges the battery to compensate for the electric energy consumed in running the electrically driven supercharger/compressor. A comprehensive model of the supercharger/turbo-generation system is assembled and interfaced with a model of a Diesel engine developed in the AMESIM multi-domain modeling environment. The model was then used to analyze both the supercharging and turbo-generation systems and to arrive at: 1) dynamic transient component performance specifications, 2) coordinated control schemes for maintaining battery state of charge and meeting transient demand on the engine, and, 3) comparison of the transient performance and fuel consumption of the proposed system with a conventional turbo-charger.

The rest of the paper is organized as follows. Section 2 describes the models developed and adopted for this study, including that of the Diesel engine, the electric motor, the generator, the battery and component controls. Section 3 outlines the coordinated control schemes. Section 4 sets up a test profile to demonstrate the functioning of the proposed system and presents demonstrative results, including a comparison with a conventionally turbo-charged engine. Finally, Section 5 summarizes the conclusions of the work.

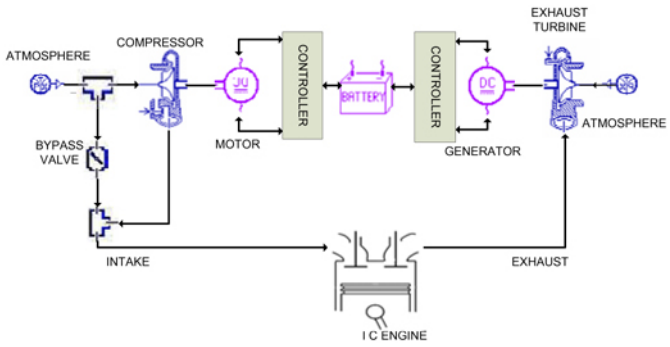

Figure 1. Schematic of the electric supercharging and turbo-generation system

2. MODEL DEVELOPMENT

The operation of the proposed system involves a multi-physical domain interaction of electrical, mechanical, pneumatic, and thermal states within and among the components of the system. Such interaction is suitably modeled with an approach grounded in Bond Graphs [9]. In this work, we adopted the commercial software AMESIM from LMS®, which allows strict enforcement of causality formulations verifiable using Bond Graphs. We used AMESIM's library of component models to construct a realistic model of the electric supercharging and turbo-generation system. In establishing the overall system model, some component level models were reduced to numerically expedient yet practical forms as will be detailed below. In addition, the simulations were executed with a variable step solver to accurately capture the dynamics of the various physical states across these domains within defined tolerances.

2.1. ENGINE MODEL

The IFP Engine library of AMESim was used to develop a model of a 4 cylinder, 2 Liter, in-line Diesel engine with a bore of 90 mm, stroke of 84 mm and compression ratio of 18:1. The model utilizes the specific crank angle degree modeling approach where all dynamic occurrences in each cylinder correspond to specified crank shaft positions [10]. The engine model uses a fixed cam profile and a constant cam phasing with respect to crankshaft position. The direct fuel injection model assumes a trapezoidal injection profile with a fixed injection phasing. The Chmela combustion model [11] is used for the thermodynamic calculations. A

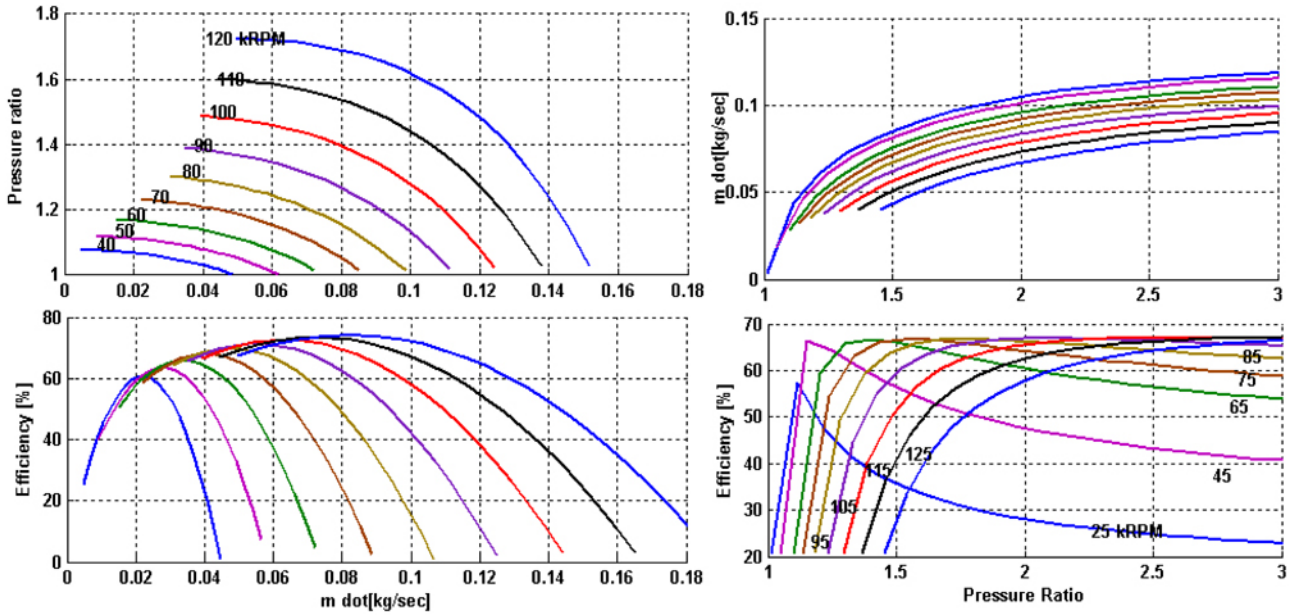

Figure 2. Compressor (left) and turbine (right, at one VGT position-50% open) performance maps

more complete description of the IFP Diesel engine model is given in [10].

2.2. COMPRESSOR AND TURBINE MODELS

The compressor and turbine were both modeled using lookup tables for their quasi-static behavior. The compressor model evaluates mass (and enthalpy) flow rates from efficiency maps. The model also simulates surge and choke limits in order to limit the effective operating range of the compressor by accounting for gas dynamics effects using fluid inertia calculations. The lookup tables for the compressor (Figure 2, left) and the turbine (Figure 2, right) selected for the proposed system were extracted from the AMESim engine library. A variable geometry turbine (VGT) was selected for the turbo-generation system in order to provide control over the regeneration regime (as will be discussed in Section 3) and for future work. However, an adequately sized turbine with a controlled waste-gate may suffice for this application. The flow behavior and energy balance were calculated using performance tables obtained from turbine maps corresponding to a number of distinct VGT actuator positions. The behavior at intermediate VGT actuator positions is determined by interpolation. To model the transient behavior in the speed dynamics of the compressor and the turbine sides, Newton's second law was applied considering the torque balance across the compressor-motor shaft or the turbine-generator shaft together with the respective gearing and rotary inertia on each shaft.

<figure 2 here>

2.3. MODELING AND SELECTION OF ELECTRICAL COMPONENTS

Increasing provisions for passenger safety, comfort and convenience functionalities continue to accelerate the increase in electrical loads on board a vehicle. This trend has led to increasing use of a 42 V bus system that enables integration of high power electrical accessories while lowering the auxiliary mechanical loads on the engine [12]. Vehicles with higher bus voltage (Electric and hybrid vehicles) may support even larger electrical accessory loads. In the present work, a 42 V electrical architecture is adopted and the system model is built assuming a dedicated 42 V Li-ion battery. However, the idea could be integrated into existing electrical systems on board a vehicle with a 42 V or higher bus voltage system provided due consideration is given to the power requirements of the proposed system.

Battery

The battery was modeled as a series interconnection of individual cells with an open circuit voltage (OCV) source and a series internal resistance (Figure 3). Both the OCV and internal resistance of the individual cells are given as functions of the state of charge (SOC) [13]. These functional characteristics (per cell) of the battery are input into the model in the form of lookup tables.

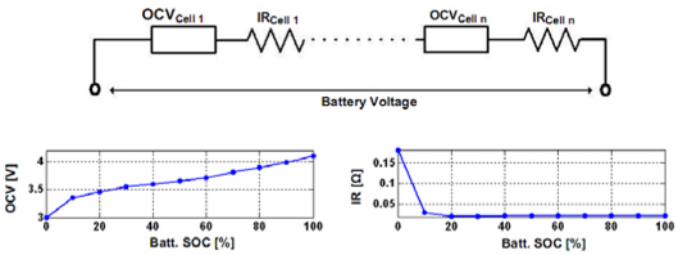

Figure 3. Schematics of battery model (top) and the characteristics for a single Li-ion cell (bottom).

Motor/Generator

A three-phase ultra high-speed permanent magnet brushless DC (PMDC) motor was selected based on the design discussed in [14] having a rated power of 2.7 kW, rated speed of 140,000 rpm and 200% overload provision. The dynamic performance parameters were tuned to suit the current electric supercharging application. For the purposes of the investigation in this paper, we also used the result from [15] that a symmetrical three-phase PMDC motor can be modeled as a single-phase DC motor with parameters satisfying some equivalence equations given therein. Then, the governing equations for the dynamics of the DC motor coupled to the compressor are given by:

$$L_a \frac{di(t)}{dt} = V_a(t) - R_a i(t) - K\omega(t) \qquad (1)$$

$$J_c \frac{d\omega(t)}{dt} = Ki(t) - D\omega(t) - T_L(t) \qquad (2)$$

where, L_a, R_a and K are the inductance, resistance and torque constant of the motor, V_a is the voltage across the armature, and, J and D are the inertia and viscous damping coefficient referred to the motor shaft. T_L is the compressor torque on the motor shaft. i is the current draw of the motor and ω is its speed.

Note that the supercharger motor can be operated in two quadrants: (1) normally, when driving the compressor as a motor and (2) the machine running as a generator to recover some of the kinetic energy during instances of low engine torque demand when the compressor is commanded to turn off and the bypass is opened. This second scenario was recognized during system simulations which showed that, during compressor turn-off and subsequent spin-down, opportunities exist for recovering the built-up kinetic energy by running the supercharger motor as a generator and recharging the battery. This possibility was taken into account in subsequent analysis.

The same ultra high-speed PMDC machine type was considered on the turbine side generator and therefore its model follows similarly. However, the generator is modeled with a causality that is the reverse of that of the motor. The adopted causality of the electro-mechanical components is shown in Figure 4 below [13].

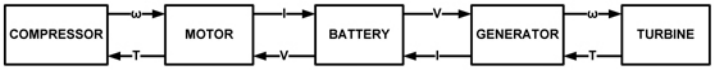

Figure 4. Flow of power factors (Causality) within the electro-mechanical components

The design parameters selected for both electric machines are given in Table 1. These values were arrived at by conducting multiple component level and subsystem level simulations to fulfill peak power and dynamic performance requirements of the proposed supercharging and turbo-generation system to work with the Diesel engine under consideration. For example, the values given in the table for the motor translate to an equivalent natural frequency 10 Hz (or an overall mechanical time constant of about 0.1 seconds) that gave satisfactory step responses on compressor turn-on. The values in the table are comparable to corresponding parameters for some commercially available machines [16].

Table 1. Design parameters of the motor and generator

Parameter	Motor/ Generator
Armature Inductance (L_a)	0.38 mH
Armature Resistance (R_a)	0.13 Ω
Machine back EMF constant (K)	0.0027 V.s/rad
Mechanical Damping coefficient (D)	$8.6\ 10^{-6}$ Nms
Mechanical Inertia (J)	$5.7\ 10^{-6}$ kgm^2

Motor/Generator Control

Control of PMDC machines is accomplished by high frequency switching of the input voltage using transistor chopper circuits. A half-bridge chopper circuit, which is suitable for the current application, can operate the DC machine as either a motor or generator [17]. The fact that the switching/chopper dynamics are much faster than the motor/ generator dynamics allows us to simplify the controller in the simulation model. If α_1 and α_2 are the chopper duty cycles in motor and generator modes, respectively, the armature voltage ($V_{a,\ motor}$) is represented by Eqs 3 and 4 [13]:

$$V_{a,motor}(t) = \alpha_1 V(t) \quad (3)$$

$$V_{a,gen}(t) = (1-\alpha_2) V(t) \quad (4)$$

A complete chopper circuit model was built in AMESIM and considered for this work. However, the simplifications in Eqs 3 and 4 gavefaster numerical solutions for the simulation of the complete Diesel engine, supercharging and turbo-generation system without noticeable difference in the results.

3. COORDINATED CONTROL SCHEME

In this section, we outline a simple control scheme that can be adopted for realizing the stated benefits of the electric supercharging and turbo-generation system. We first describe the load control scheme for the Diesel engine considered for this study. This is then followed by a description of the control scheme for both the compressor/supercharger and the turbine/generator sides.

3.1. ENGINE FUEL FLOW CONTROL

A closed loop speed controller manipulates the fuel flow rate in response to changes in power demand. Injection timing is kept constant for this study. Engine power demand is governed by the load torque and speed of the crankshaft. At a particular point, if load torque increases, the speed of the crankshaft reduces, to which the engine controller responds by increasing the fuel quantity injected. The engine controller used is a PI controller regulating crankshaft speed to desired speeds specified in the drive cycle. The control action (injection quantity) is then saturated with a (varying) maximum fuel flow rate that keeps the air excess factor λ higher than the smoke limit for the prevailing intake air mass flow rate (which is assumed to be measured with a MAF sensor or estimated).

In the subsequent discussion of engine load, the air/fuel ratio (or the excess air factor λ) determined by the engine controller is taken as the main indicator of load for Diesel engines. High λ indicates light load, while low λ approaching the smoke limit indicates high load.

3.2. SUPERCHARGER AND TURBO-GENERATOR CONTROL

The control scheme for the proposed system is outlined in Figure 5. The two major monitored variables are the state of charge (SOC) of the battery and the engine load. The air/fuel ratio given by λ is determined from the fuel-injection control scheme. Since a dedicated battery is considered, its SOC at any time must be such that: 1) it can continue to accept power from turbo-generation or compressor spin-down, and, 2) it can provide power to the compressor motor without depleting SOC reserves. These considerations define the SOC window of operation between a low, SOC_{low}, below which the compressor-motor should be turned off and a high SOC_{high}, above which the turbo-generator should be essentially wide open (no re-generation). Based on battery efficiency considerations SOC_{low} = 40% (Figure 3, internal resistance). The upper limit is set at SOC_{high} = 90% in order to leave margins against over-charging the battery.

Engine load considerations suggest different operating regimes for the supercharger and the turbo-generator. At higher load demand near the smoke limit, compressor activation is desirable. During this regime, the VGT actuators of the turbine should be wide-open so as not to build back-pressure in the exhaust, increase pumping losses and thereby counteract the compressor action. At lower load, where supercharging is not needed, the turbo-generator should be activated to recuperate some of the exhaust energy and use it to recharge the battery.

3.2.1. Compressor Control

The supercharger/compressor operation is controlled by switching the supply voltage to the electric motor via the chopper duty cycle, α_1. The switching thresholds are set based on the output of the engine controller, which determines the fuel injection in response to load changes. In the present work, the thresholds are set at pre-determined air/fuel ratio or λ set-points (Figure 5). When fuel injected becomes greater than the fuel required to maintain a particular λ value, $\lambda_{On,Comp}$, the compressor motor is switched ON. When the motor is turned ON, the compressor is speed-controlled (with a PID loop manipulating the chopper duty cycle) to operate at a pre-selected optimal efficiency speed set point determined from the compressor map (Figure 2). For subsequent simulations the compressor set speed is maintained at 80,000 rpm. The compressor tries to lean out the mixture by increasing the air mass flow rate in response to increasing fuel injection (load) and allow the engine to respond with higher torque from increased volumetric efficiency and without running into the smoke limit. When fuel demand drops below the fuel quantity required to maintain a particular lean λ value, $\lambda_{Off,Comp}$, the voltage supply to the compressor motor is switched OFF and the intake by-pass valve is immediately opened wide for the engine to aspirate naturally. Note that with a variable speed electric motor, the compressor output may also be manipulated by varying the speed set point to vary intake mass flow rate as a function of engine operating point. However, here, we have adopted the simplified control scheme above (where the compressor is regulated at the optimal speed set point after turn on) to first demonstrate the feasibility of the proposed system.

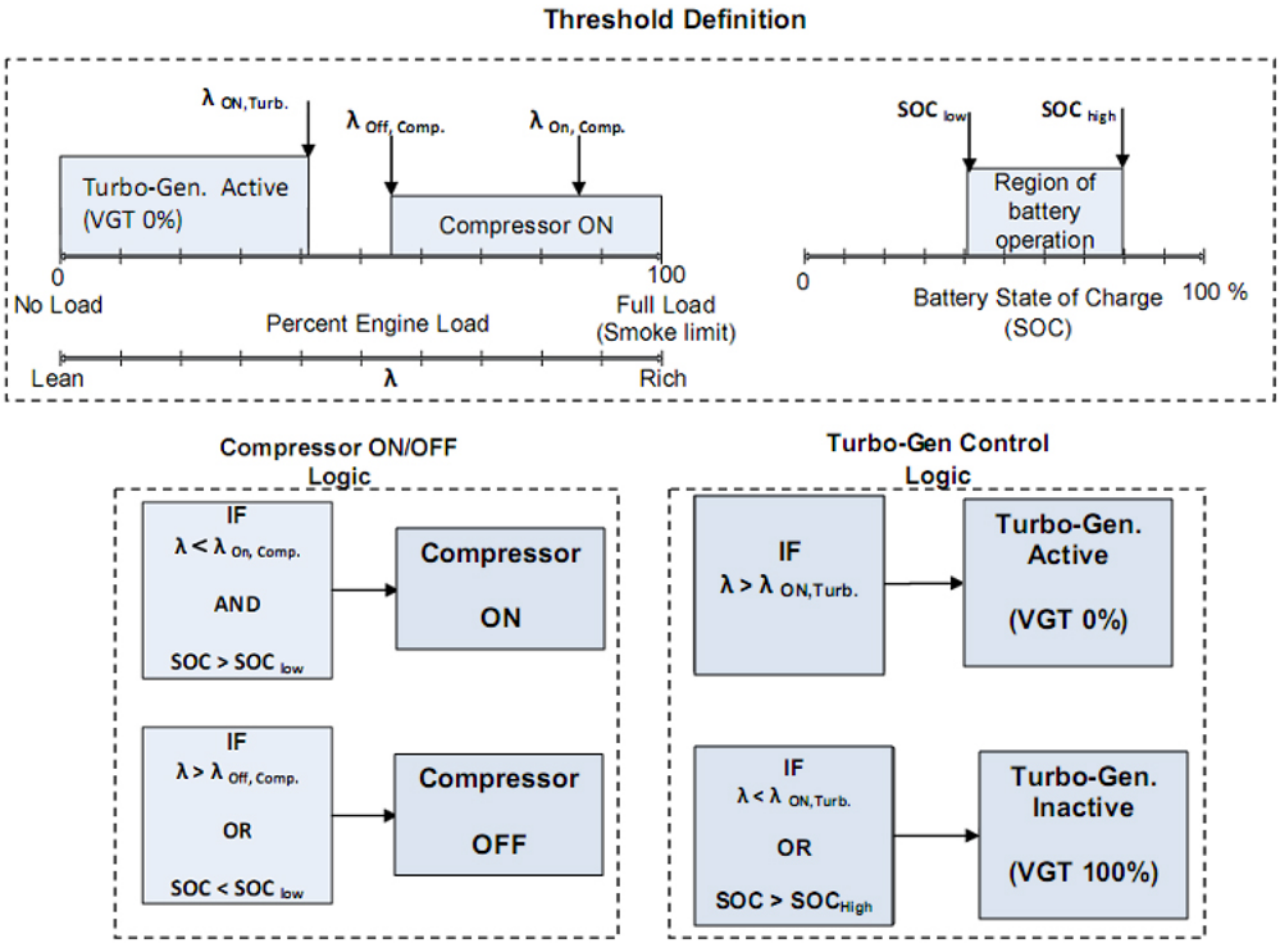

Figure 5. Schematic of load and SOC based control of the supercharger and turbo-generator

<figure 5 here>

Battery state of charge (SOC) considerations will override the above engine-load based control of the compressor motor. If the dedicated battery is discharged below a certain threshold (SOC_{low}), the compressor motor should not be turned on. To minimize such events, which will reflect as unsatisfactory acceleration performance for the engine, the turbo-generator control must strive to charge the dedicated battery whenever possible. Furthermore, as will be shown in the next section, for a given drive cycle, changing the compressor ON/OFF thresholds, $\lambda_{ON,Comp}$ and $\lambda_{OFF,Comp}$, changes the duration for which the compressor remains ON. This indicates further possibility for dynamically varying these thresholds to preserve the SOC of the battery depending on the operating cycle.

3.2.2. Turbine Control

The variable geometry turbine (VGT) considered here allows us to alter the pressure drop across the turbine by changing the position of the VGT actuator thereby achieving control over the torque output of the turbine. As in conventional turbochargers, for the turbo-generator application, control of exhaust back pressure should be connected to engine demand, i. e. the air-fuel ratio (or λ). As pointed out above (Figure 5), with increasing load beyond $\lambda_{ON,Turb}$, the VGT should impose the least exhaust back pressure (VGT wide open, Turbo-generator inactive) to minimize pumping losses. On the other hand, when engine load is lower than $\lambda_{ON,Turb}$, the VGT increases back pressure (the VGT restriction maximum, Turbo-generator active) thereby generating more torque on the generator shaft. This allows for recuperating exhaust heat via the generator charging the battery. Note that this scheme is rather effective in highway driving with plenty of low-load opportunities for recovering energy from the exhaust.

Again, the battery SOC will override the engine load-based control of the turbo-generator. For a dedicated battery, if the SOC is higher than a given threshold (say, 90%), there is no more room for storing recovered energy and in this situations the VGT should be left wide open (Turbo-generator inactive). All the controller set points were selected using an iterative process to attain optimum system performance as discussed below.

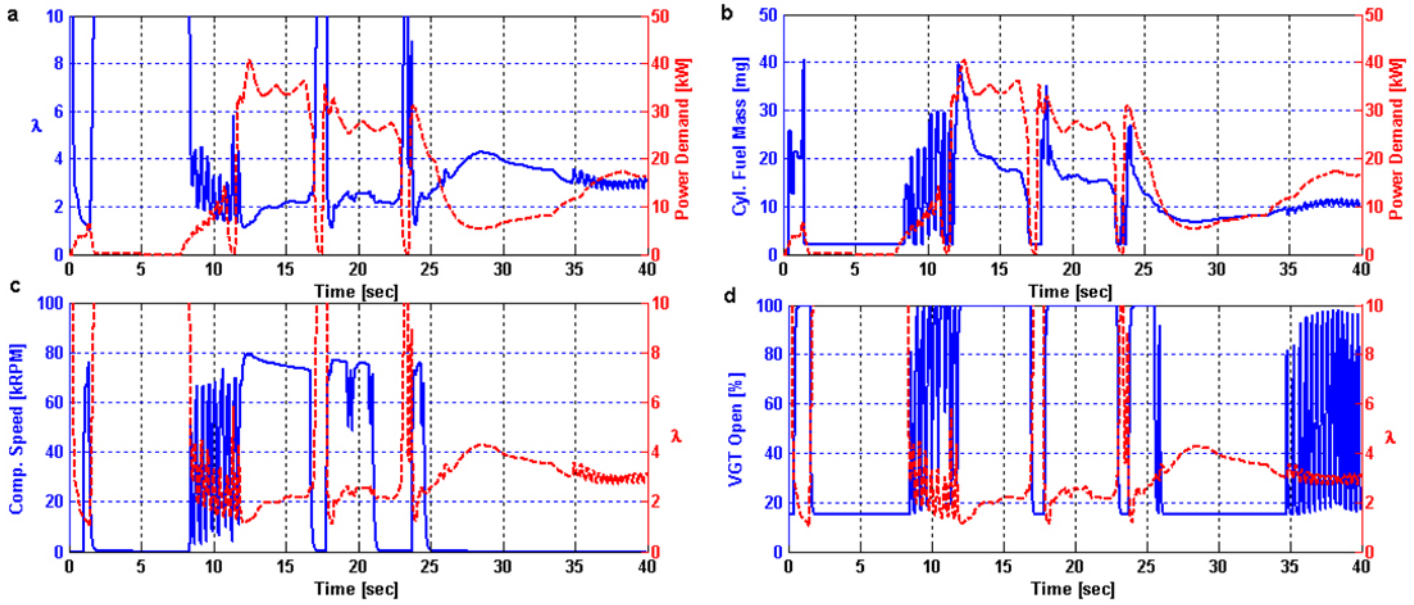

Figure 7. Demonstration of system performance over a portion of the FUDS cycle

4. RESULTS AND DISCUSSIONS

4.1. DEMONSTRATIVE TEST PROFILE

A passenger car model was developed using the AMESim Drive library [18] to determine engine load and speed demand data corresponding to the vehicle speed profile of the Federal Urban Drive Schedule (FUDS). Highly transient sections of this test cycle have been extracted for the purpose of developing and experimenting with the control strategy discussed above. An illustration of the engine speed and torque data corresponding to a transient section of the FUDS between 180 to 220 seconds is shown in Figure 6.

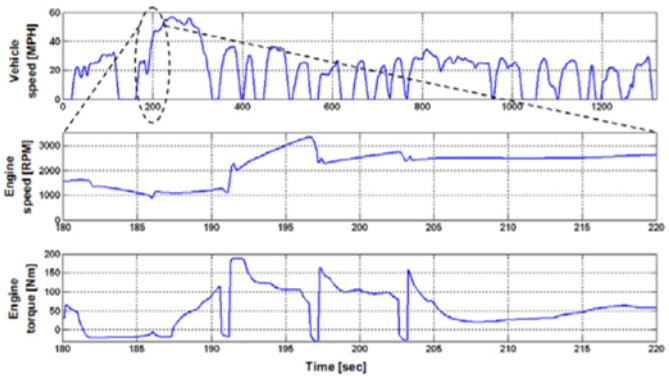

Figure 6. Engine speed and torque data for a transient section of the FUDS test cycle

4.2. SYSTEM PERFORMANCE

The simulated response of the system during the 40 second interval starting at the 180th second is shown in Figure 7. The control thresholds were set as: $\lambda_{ON,Comp}$= 1.67, $\lambda_{OFF,Comp}$= 2.67, $\lambda_{ON,Turb}$= 3.0. Figure 7a justifies the selection of λ to represent engine power demand. Figure 7b shows the fuel mass injected in each cylinder per cycle determined by the fuel flow controller corresponding to engine power demand. These two figures simply verify the intended operation of the engine controller as described in Section 3.1

Figure 7c demonstrates the implementation of the compressor control strategy over the same 40 second interval. The motor spins up the compressor to its set speed of 80,000 rpm whenever λ drops below $\lambda_{ON,Comp}$. It maintains the set speed as long as the A/F mixture remains rich in response to high power demand. Figure 7d shows the turbine geometry control for the same interval. Note that the controller avoids exhaust back pressure build up during high load engine operation by leaving the VGT wide-open. At low engine power demands (i. e. high λ), the controller restricts the VGT opening to increase the turbine torque on the generator which in turn increases the battery charge current.

<figure 7 here>

4.3. SELECTION OF CONTROLLER THRESHOLD POINTS

The current drawn by the compressor motor and the change in battery SOC with two different turn-ON threshold points are depicted in Figure 8a-b. For the results in Figure 8, the turbo-generator is kept inactive. When the compressor is commanded to turn ON at a lower engine load (higher threshold), the battery SOC depletes faster (Figure 8c) without significant improvement in transient response (Figure

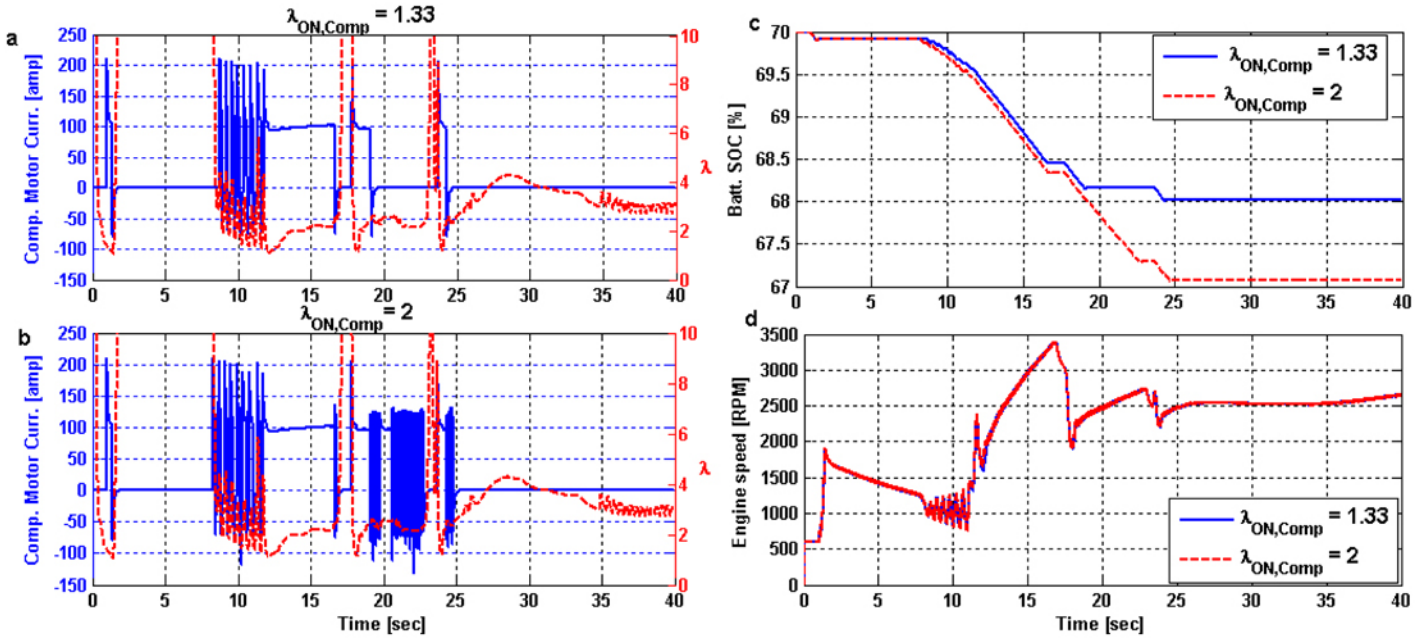

Figure 8. Compressor control threshold points selection

8d). This result indicates that intake pressure boost in Diesel engines is effective only during peak load conditions. Under part load conditions, the engine runs lean and intake boost is unnecessary. It should be noted that SOC depletion magnitudes shown in Figure 8c are small due to the modest time duration considered for the plots.

Similar analysis conducted for compressor turn-OFF threshold indicates that due to large variation of λ in Diesel engines, oscillations may occur in ON/OFF switching of the compressor. However, by selection of a wider operating window for the compressor, the oscillations can be reduced at the expense of depleting the battery SOC at a faster rate. For the present system, after conducting numerous iterations, the optimal values for $\lambda_{ON,Comp}$= 1.67 and $\lambda_{OFF,Comp}$= 2.67 were selected and used for subsequent analysis.

<figure 8 here>

The turbo-generator threshold point ($\lambda_{ON,Turb}$) was selected based on an analysis similar to compressor threshold point selection. Figure 9 shows the current generated by the turbo-generator for two turbo-gen. activation threshold points. If the turbo-gen. activation point is pushed to lower λ values (higher load), the energy recovery opportunities of the turbo-generator widen. In this case, the turbo-generation begins earlier as engine load is being removed. However, beyond a certain point, the exhaust back-pressure created affects the engine performance adversely by increasing the pumping losses. Considering this trade-off, the optimal value of $\lambda_{ON,Turb}$=3.0 was selected for subsequent analysis.

<figure 9 here>

4.3. COMPARISON WITH A CONVENTIONAL TURBO-CHARGER

To compare the proposed supercharging and turbo-generation system with a conventional turbo-charging system, a similar simulation model was developed for the conventional system fitted to an identical Diesel engine. All engine related settings (injection timing, load control) were kept the same for the two cases. As shown in Figure 10 (left), the engine with the proposed electric supercharging system responds faster to large demanded speed changes. This is enabled by the almost instant turn-on of the compressor and the wide-open VGT gates, which offer minimal back-pressure buildup during the high load transient. The turbo-charger on the other hand relies on exhaust back-pressure build up to accelerate the compressor and provide boost to the engine. The proposed system virtually eliminates the so-called turbo-lag. It can also be seen in Figure 10 (right) that during the transient, more fuel is used by the turbocharged engine. However, the proposed system also uses battery energy during the maneuver and a true comparison of fuel use should look at the fuel consumption over a dedicated test cycle, as we will do below.

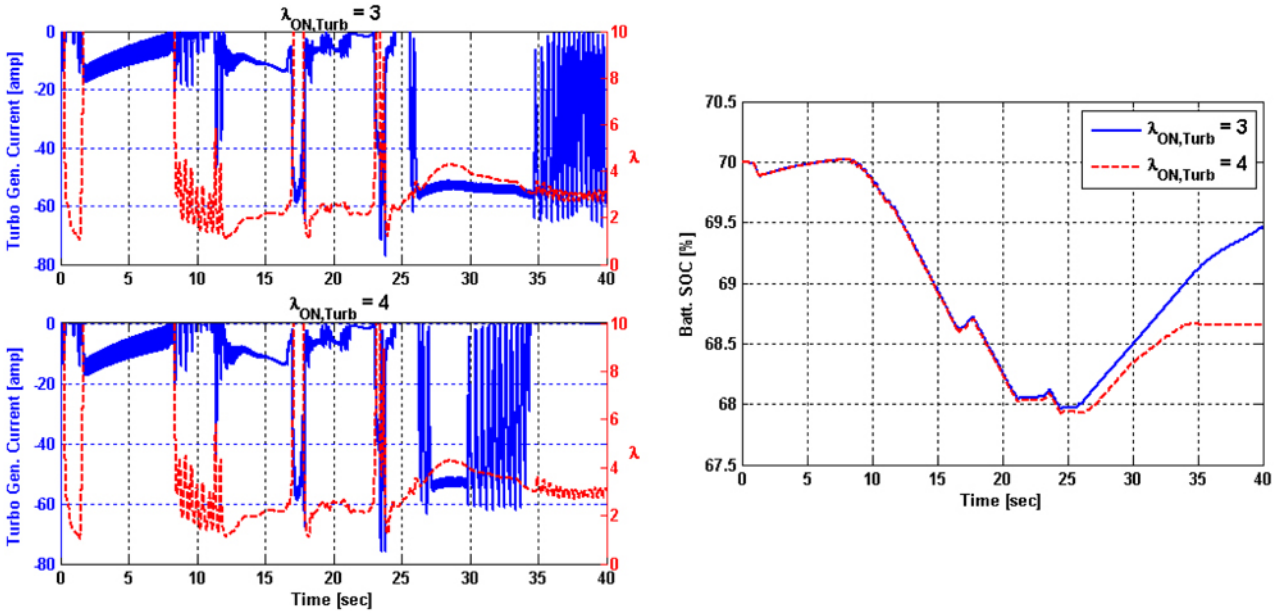

Figure 9. Turbo-generator threshold point selection

Table 2. Fuel use and energy output comparisons over a segment of FUDS test cycle

	EPA FUDS		EPA Highway Fuel Economy Test Schedule	
	Proposed Electric Supercharging System	Conventional Turbocharged System	Proposed Electric Supercharging System	Conventional Turbocharged System
Fuel mass used (grams)	466	482	513	480
Calculated miles/gallon	51.6	49.9	64.9	69.3
Battery energy recuperated (W-hr)	62.3	-	138	-
Total equivalent fuel used (grams)	450	482	478	480
Equivalent MPG	53.4	50	69.7	69.3

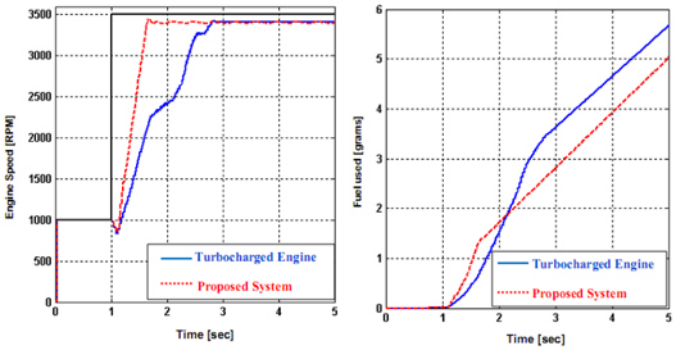

Figure 10. Comparison of transient response between the proposed system and conventional turbocharger

<table 2 here>

The simulation results of the conventional turbocharged engine and the proposed system over the entire EPA FUDS and EPA HWFET (highway fuel economy test) are summarized in Table 2 above. As discussed earlier, the electric energy recuperated into the energy buffer during these tests can be attributed to generation on the turbine side and regeneration during compressor spin-down. Energy recovered during compressor spin-down accounted for 16% and 2% of total energy recovered over the FUDS and highway tests, respectively. For comparing the energy efficiency of the proposed system with the conventionally turbo-charged system, the electric energy regenerated/drawn into/from the battery should be accounted for converting it into equivalent fuel energy that would be saved/used by using this system during future transients. From the simulation results, it is evident that the proposed system exhibits a nearly 7% improvement in overall fuel efficiency over the FUDS. This is due to frequent transient operation in this cycle. However, over the EPA highway test cycle, the electric supercharging system is inoperative almost all the time due to mostly steady-state operation of the engine. Here, the engine runs naturally aspirated on the intake side while the exhaust flow is restricted by the turbo-generator. This increases back-pressure on the exhaust side resulting in increased pumping losses and higher fuel consumption. This offsets the energy recovery by the turbo-generator, thereby minimizing equivalent fuel consumption improvement on the highway cycle.

5. CONCLUSIONS

A model of an electric supercharging and turbo-generation system has been developed and causally integrated with the model of a Diesel engine and of a dedicated energy storage system (battery). Then, component dynamic performance specifications have been identified and a coordinated control scheme is proposed that considers engine load and battery state of charge to set operating regimes for the supercharger and the turbo-generator. Operating thresholds have also been identified for the coordinated control scheme using extensive system simulations.

It is argued that the proposed system has distinct transient response improvement benefits over a conventional turbo-charged system. It is possible to virtually eliminate the so-called turbo-lag in the response of the engine to large demanded-speed transients. Furthermore, during transients and high load operation, the proposed system does not build up exhaust backup pressure in order to accelerate the supercharger and as such does not incur additional pumping losses. This, and the fact that electrical energy that is consumed by the supercharger can be partially obtained from exhaust waste heat recovered via turbo-generation during low

load operation, improves the overall efficiency of the engine fitted with the proposed system. Over the FUDS cycle, apart from the better transient behavior of the engine, equivalent fuel consumption comparisons with a similar engine fitted with a conventional turbocharger showed about a nearly 7 % improvement for the engine fitted with the proposed system. Better fuel efficiency also suggests an improvement in emissions during transient engine operation (a major concern with conventional diesel engines). The efficiency improvement is, however, absent during low-load steady-state operation over the highway test cycle where energy stored in the buffer increases at the expense of reduced fuel efficiency from increased back-pressure and pumping losses.

More research is being pursued to determine whether the identified improvement in engine performance can justify the added cost and weight of the multiple electrical components (DC motor and generator, battery and power electronics). The control strategies need further optimization to maximize the benefits under the proposed overall scheme. There are also opportunities to integrate this system into the overall electrical system of the vehicle along with possible downsizing of the alternator by replacing some of its function or energy supply with that coming from the turbo-generator of this proposed system. Disparities between the battery charging/discharging efficiencies, and influences on battery life need to modeled and understood. Another important aspect often employed to mitigate NO_X emissions with Diesel engines, is the use of EGR (exhaust gas recirculation). The coordinated control of EGR together with the proposed system, particularly in transient operating modes, needs to be addressed. These issues will form part of our future work.

REFERENCES

1. Ecker, H.-J., Schwaderlapp, M., and Gill, D. K., "Downsizing of Diesel Engines: 3-Cylinder / 4-Cylinder," SAE Technical Paper 2000-01-0990, 2000.

2. Guzzella, L. and Onder C. H., *Introduction to Modeling and Control of Internal Combustion Engine Systems*, 2004, Berlin, Springer.

3. Lee, B., Filipi, Z., Assanis, D., and Jung, D., "Simulation-based Assessment of Various Dual-Stage Boosting Systems in Terms of Performance and Fuel Economy Improvements," *SAE Int. J. Engines* 2(1):1335-1346, 2009.

4. Pallotti, P., Torella, E., New, J., Criddle, M. et al., "Application of an Electric Boosting System for a Small, Four-Cylinder S.I. Engine," SAE Technical Paper 2003-32-0039, 2003.

5. George, S., Morris, G., Dixon, J., Pearce, D. et al., "Optimal Boost Control for an Electrical Supercharging Application," SAE Technical Paper 2004-01-0523, 2004.

6. Hoecker, P., Jaisle, W., and Munz, S., "The eBooster from BorgWarner Turbo Systems - The key Component for an Automobile Charging System," BorgWarner Turbo Systems-Academy Technical Literature.

7. Michon, M., Calverley, S. D., Clark, R. E., Howe, D., Chambers, J.D.A., Sykes, P.A, Dickinson, P.G., Clelland, M.M., Johnstone, G., Quinn, R., and Morris, G., "Modelling and Testing of a Turbo-Generator System for Exhaust Gas Energy Recovery", 2007 IEEE Vehicle Power and Propulsion Conference, Sept 9-12, pp 544-550, Arlington, TX.

8. Calverley, S.D., Jewell, G.W., and Saunders, R.J., "Design of a High Speed Switched Reluctance Machine for Automotive Turbo-Generator Applications," SAE Technical Paper 1999-01-2933, 1999.

9. Karnopp, D.C., Margolis, D.L., and Rosenberg R.C., *Systems Dynamics: a Unified Approach*, 1990, John Wiley & Sons, New-York.

10. IFP Engine Library 2007, LMS Imagine.Lab AMESIM Software documentation.

11. Chmela, F.G. and Orthaber, G.C., "Rate of Heat Release Prediction for Direct Injection Diesel Engines Based on Purely Mixing Controlled Combustion," SAE Technical Paper 1999-01-0186, 1999.

12. Kassakian, J. G., "Automotive Electrical Systems-the Power Electronics Market of the Future," Fifteenth Annual IEEE Applied Power Electronics Conference and Exposition APEC 2000, Feb 6-10, Vol.1, pp3-9, New Orleans, LA.

13. Guzzella, L. and Sciarretta, A., *Vehicle Propulsion Systems: Introduction to Modeling and Optimization*, 2007, Springer.

14. Noguchi, T., Takata, Y., Yamashita, Y. and Ibaraki, S., "160,000 r/min, 2.7 kW Electric Drive of Supercharger for Automobiles", Proceedings of the International Conference on Power Electronics and Drive Systems, Vol. 2, pp 1380-1385, 2005

15. Pan, C.T. and Fang, E., "A Phase-Locked-Loop-Assisted Internal Model Adjustable-Speed Controller for BLDC Motors", IEEE Transactions on Industrial Electronics, Vol. 55. No. 9, pp 3415-3425, 2008.

16. Toliyat, H.A. and Kliman, G.B., "*Handbook of Electric Motors*", 2004: Marcel Dekker, Inc.

17. Rashid, M.H., *Power Electronics Handbook: Devices, Circuits and Applications*, 2001, San Diego, Academic Press.

18. IFP-Drive Library Manual. 2007: LMS Imagine.Lab AMESIM Software Documentation.

CONTACT INFORMATION

Dr. Beshah Ayalew
International Center for Automotive Research
4 Research Dr., Room 342 CGEC
Greenville, SC 29650, USA.
beshah@clemson.edu
Phone: 864-283-7228.

The Engineering Meetings Board has approved this paper for publication. It has successfully completed SAE's peer review process under the supervision of the session organizer. This process requires a minimum of three (3) reviews by industry experts.

ISSN 0148-7191

doi:10.4271/2010-01-1228

SAE Customer Service:
Tel: 877-606-7323 (inside USA and Canada)
Tel: 724-776-4970 (outside USA)
Fax: 724-776-0790
Email: CustomerService@sae.org
SAE Web Address: http://www.sae.org
Printed in USA